

# Bound Magnetic Polaron Interactions in Insulating Doped Diluted Magnetic Semiconductors

Adam C. Durst<sup>1,2</sup>, R. N. Bhatt<sup>1</sup>, and P. A. Wolff<sup>2</sup>

<sup>1</sup>*Department of Electrical Engineering, Princeton University, Princeton, New Jersey 08544*

<sup>2</sup>*Department of Physics, Massachusetts Institute of Technology, Cambridge, Massachusetts 02139*

(October 24, 2018)

The magnetic behavior of insulating doped diluted magnetic semiconductors (DMS) is characterized by the interaction of large collective spins known as bound magnetic polarons. Experimental measurements of the susceptibility of these materials have suggested that the polaron-polaron interaction is ferromagnetic, in contrast to the antiferromagnetic carrier-carrier interactions that are characteristic of nonmagnetic semiconductors. To explain this behavior, a model has been developed in which polarons interact via both the standard direct carrier-carrier exchange interaction (due to virtual carrier hopping) and an indirect carrier-ion-carrier exchange interaction (due to the interactions of polarons with magnetic ions in an interstitial region). Using a variational procedure, the optimal values of the model parameters were determined as a function of temperature. At temperatures of interest, the parameters describing polaron-polaron interactions were found to be nearly temperature-independent. For reasonable values of these constant parameters, we find that indirect ferromagnetic interactions can dominate the direct antiferromagnetic interactions and cause the polarons to align. This result supports the experimental evidence for ferromagnetism in insulating doped DMS.

PACS numbers: 75.50.Pp, 75.10.-b, 75.30.Hx

## I. INTRODUCTION

Diluted magnetic semiconductors (DMS) are semiconductors in which a fraction of the nonmagnetic ions that make up the crystal structure have been replaced by magnetic transition metal or rare earth ions. For example, substituting  $\text{Mn}^{2+}$  ions for some of the Cd ions in the nonmagnetic semiconductor, CdTe, yields the diluted magnetic semiconductor,  $\text{Cd}_{1-x}\text{Mn}_x\text{Te}$ . In doped DMS, the sizable exchange interaction between magnetic ions and carriers (electrons or holes) leads to unusual optical, magnetic, and transport properties. Due to their potential for use in novel devices which take advantage of both their semiconducting and magnetic properties, DMS have, of late, been the subject of much interest.<sup>1,2</sup> Recently, the discovery<sup>3</sup> of a ferromagnetic transition temperature of 110 K in a sample of  $\text{Ga}_{1-x}\text{Mn}_x\text{As}$  with  $x \approx 0.05$  has further enhanced both the experimental<sup>4-8</sup> and theoretical<sup>9-15</sup> interest in DMS.

In the II-VI DMS  $\text{Zn}_{1-x}\text{Mn}_x\text{Te}$  ( $x \leq 0.1$ ), p-doped with carriers at the level of  $3 \times 10^{17}/\text{cm}^3$ , where the system is in the insulating state, measurements of susceptibility versus applied magnetic field were conducted by J. Liu at NEC Research Institute. The data, originally reported in an NEC technical memo<sup>16</sup>, has been reproduced in Fig. 1 for the convenience of the reader. Note the double-step structure of the susceptibility and the two characteristic field scales indicated by the inflection points of the curve. This form suggests a dual magnetization mechanism whereby large collective spins align at fields ( $\sim 300$  G) too weak to magnetize the individual magnetic ions. Only at much larger fields ( $\sim 15,000$  G) do the individual Mn spins align. Within this interpretation, the measured susceptibility can be viewed as the

sum of two contributions: a collective spin term that drops off around 300 G and an individual spin term that drops off around 15,000 G. The dashed line in Fig. 1 serves to separate these two contributions.

For the  $x$ -regime in question, the Mn concentration is not enough to percolate, and the undoped system is not magnetically ordered. (Spin glass type order of the undoped system has been observed in II-VI DMS for Mn concentrations above  $x = 0.2$ .<sup>17</sup>) Consequently, the unusual magnetic behavior is attributable to the presence of the dopants. This is not surprising, despite the low carrier concentration, because the Bohr radius which characterizes the carrier wave function is large compared to the Mn 3d wave function which characterizes the extent of the Mn local moment. We interpret the large collective spins, responsible for the double-step form of the susceptibility, to be bound magnetic polarons, formed by the exchange interaction between localized carriers and magnetic ions within the carrier orbit. Furthermore, a fit of the polaron part of the the susceptibility data to a Curie-Weiss form reveals a net ferromagnetic interaction between the polarons. This result is in stark contrast to that observed for conventional nonmagnetic semiconductors in which virtual carrier hopping invariably yields antiferromagnetism.<sup>18</sup> To explain both the formation of bound magnetic polarons and the ferromagnetic nature of their interaction, we introduced, in Ref. 19, a bound magnetic polaron model for insulating doped DMS. This was further elucidated by a comprehensive calculation in which we showed how the parameters of the model could be obtained in an optimal manner using a variational principle<sup>20</sup>, which we present below.

In Sec. II, we describe the system of two interacting polarons in a diluted magnetic semiconductor and develop

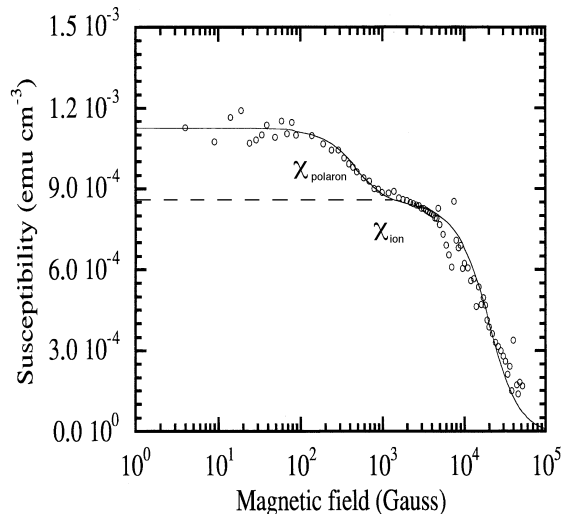


FIG. 1. Magnetic susceptibility ( $dM/dH$ ) of  $\text{Zn}_{1-x}\text{Mn}_x\text{Te}$  ( $x \approx 0.1$ ), p-doped at the level of  $3 \times 10^{17}/\text{cm}^3$ , measured at 2 K as a function of applied magnetic field. Circles denote measured data while the solid line is a fit to a dual magnetization model. The dashed line separates the collective spin (polaron) contribution from the individual Mn spin contribution. Data was obtained by J. Liu<sup>16</sup> at NEC Research Institute and is reproduced here with the permission of NEC.

a simplified model to capture its behavior. In Sec. III, we calculate, within our model, both the single polaron partition function and the polaron-pair partition function. Making use of these partition functions, we implement a variational procedure, in Sec. IV, to optimize the parameters of our model. We find that while the model parameters describing single polaron formation are temperature-dependent, the polaron-polaron interaction parameters can be treated as temperature-independent constants for magnetic ion and carrier densities of interest. We make use of these results in Sec. V where we demonstrate how a ferromagnetic polaron-polaron interaction can come about. Conclusions are presented in Sec. VI.

## II. POLARON-PAIR SYSTEM AND MODEL

### A. The System

To understand the magnetic behavior of diluted magnetic semiconductors, we consider the polaron-pair system which consists of two carriers (electrons or holes) bound to impurity sites (donors or acceptors) separated by an inter-impurity distance,  $R_{12}$ , and the magnetic ions (usually spin 5/2 Mn) which surround them. This complex system interacts via three independent exchange interactions each of which have different characteristic length scales.

The bound carriers interact directly via an impurity-impurity exchange interaction. Although this interaction can be more complicated for the case of acceptors (for which the valence band is degenerate)<sup>21</sup>, we assume an impurity-impurity interaction of the Heisenberg type, as in the donor case, characterized by an exchange constant  $J$ . This interaction has been shown to be antiferromagnetic for donors in nonmagnetic semiconductors<sup>18</sup> and is assumed to be so for carriers in diluted magnetic semiconductors as well.  $J$  is a function of the inter-impurity distance and the effective Bohr radius and varies as

$$J \sim \exp(-2R_{12}/a_B). \quad (2.1)$$

Were it not for the influence of additional interactions, this direct exchange would yield a net antiferromagnetic exchange interaction in DMS.

The second interaction at work in this system is the exchange interaction between each of the carriers and the magnetic ions. This interaction is also antiferromagnetic and is proportional in magnitude to  $\alpha|\Psi|^2$  where  $\alpha$  is the carrier-ion exchange constant for the particular material and  $\Psi$  is the carrier wave function. For the purpose of this study, we will take  $\Psi$  to be the hydrogenic wave function

$$\Psi(\mathbf{r}) = (\pi a_B^3)^{-1/2} \exp(-r/a_B) \quad (2.2)$$

with an effective Bohr radius  $a_B$ . However, it should be noted that for acceptors in particular, the carrier wave functions may be more complicated.<sup>22</sup> We are also implicitly assuming that the binding energy of the impurity is large compared to the magnetic energy of the polaron, so magnetic ordering does not change the carrier wave function.

Finally, there exists an additional antiferromagnetic exchange interaction, between the individual magnetic ions, which has a characteristic length scale on the order of a magnetic ion radius ( $\sim \text{\AA}$ ). Since this length scale is small compared with others in the system (i.e.  $a_B \sim 10 - 20\text{\AA}$ ), we neglect all but nearest neighbor interactions and assume that the nearest neighbors form inert singlets. Thus, ion-ion interactions are considered only via the use of an effective magnetic ion concentration,  $\bar{x} \equiv x(1-x)$ <sup>12</sup>, in place of  $x$ , the true magnetic ion concentration.<sup>17</sup>

Hence, the polaron-pair system (given the assumptions noted above) interacts via two antiferromagnetic exchange interactions, a carrier-carrier interaction and a carrier-magnetic ion interaction. These interactions are depicted in Fig. 2 and result in the Hamiltonian

$$H = \alpha \sum_n \mathbf{s}_1 \cdot \mathbf{S}_n |\Psi_{1n}|^2 + \alpha \sum_n \mathbf{s}_2 \cdot \mathbf{S}_n |\Psi_{2n}|^2 + J_{\mathbf{s}_1} \cdot \mathbf{s}_2 \quad (2.3)$$

where  $n$  runs over all magnetic ions,  $\Psi_{1n}$  and  $\Psi_{2n}$  are the carrier wave functions at the magnetic site  $n$ ,  $\mathbf{s}_1$  and  $\mathbf{s}_2$  are the carrier spins, and the  $\mathbf{S}_n$  are magnetic ion spins.

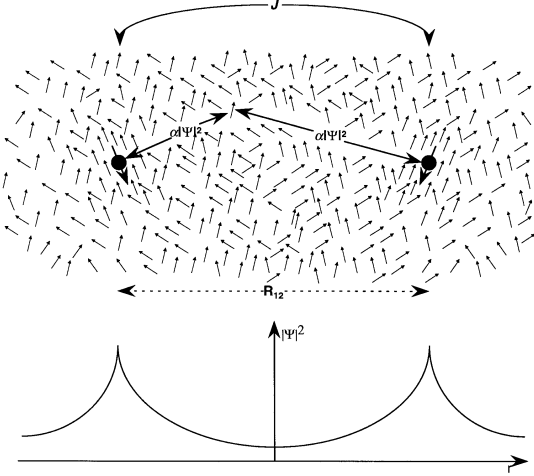


FIG. 2. Schematic of polaron-pair system.

We consider this to be a polaron-pair system because carrier-ion interactions tend to anti-align the spins of magnetic ions in the vicinity of a carrier with respect to the carrier spin. Thus, each carrier and the ions in its vicinity form a single magnetic polaron with a large collective spin. The polarons interact via both the direct antiferromagnetic carrier-carrier exchange interaction and the indirect ferromagnetic exchange interaction that results when carrier-ion interactions cause both polarons to anti-align with the same magnetic ions. Details of the competition between these two interactions will be explored as we study the nature of a simplified model.

### B. The Model

Although the true Hamiltonian provides the best description of the polaron-pair system, its solution is complicated by the fact that the magnitude of the carrier-ion interaction varies exponentially with carrier-ion distance (since carrier wave functions are hydrogenic). In order to obtain a more detailed understanding of the polaron-pair system, it is necessary to study a simplified, more tractable model. Such a model is obtained by making two simplifying approximations: the single step approximation and the interstitial region approximation.

The single step approximation entails replacing the carrier wave functions by radial step functions that are constant up to a radius  $R$  and zero beyond  $R$ . In this approximation, all of the magnetic ions within a sphere of radius  $R$  about a carrier interact with that carrier with the same exchange constant,  $K$ . Thus, in this model, the definition of a polaron becomes clear. A polaron is composed of a single carrier and all of the magnetic ions within a radius  $R$  of the impurity site to which the carrier is bound. This approximation, first developed by Ryabchenko and Semenov<sup>23</sup>, allows for the exact calcu-

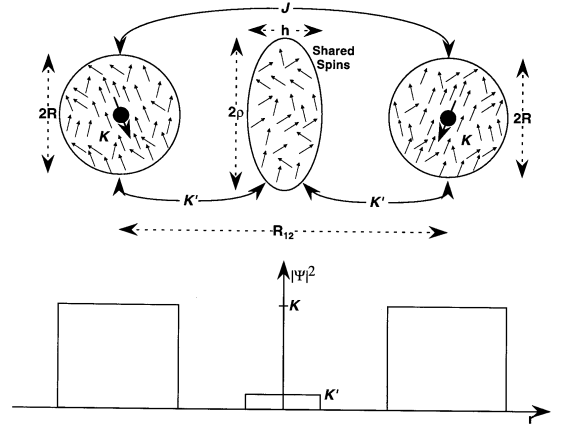


FIG. 3. Schematic of polaron-pair model.

lation of the single polaron partition function and makes the polaron-pair case much more tractable.

To consider interactions between two polarons, we must make the additional conjecture that there is an interstitial region between the two polarons within which the magnetic ions interact significantly with both carriers. Such a region must exist in order for the indirect ferromagnetic carrier-ion-carrier interactions to be significant. In order to treat the effects of these interstitial ions within our model, we assume a cylindrically symmetric interstitial region within which all of the magnetic ions interact with both of the carriers with an exchange constant,  $K'$ . In this interstitial region approximation<sup>24</sup>, carrier-ion exchange causes both carrier spins to anti-align with the interstitial spins and thereby align with each other. Thus, an indirect source of carrier-carrier ferromagnetism is introduced into the model.

In the end, the above approximations yield the model Hamiltonian

$$H_m = K [(s_1 \cdot S_1) + (s_2 \cdot S_2)] + K' (s_1 + s_2) \cdot S_3 + J s_1 \cdot s_2 \quad (2.4a)$$

$$S_1 \equiv \sum_{\text{Sphere \# 1}} S_i \quad S_2 \equiv \sum_{\text{Sphere \# 2}} S_j \quad S_3 \equiv \sum_{\text{Interstitial}} S_k \quad (2.4b)$$

where  $K$  is the intra-polaron ion-carrier exchange constant,  $K'$  is the interstitial ion-carrier exchange constant,  $J$  is the direct carrier-carrier exchange constant,  $s_1$  and  $s_2$  are the carrier spins,  $S_1$  and  $S_2$  are the net polaron spins, and  $S_3$  is the collective spin of the interstitial region. (At this point, we specify only that the interstitial region have cylindrical symmetry and be located between the polarons. However, for computational purposes, a particular shape must be chosen. This matter is discussed further in Sec. IV B.) As is indicated in Fig. 3 where the details of this model are presented graphically,

the essence of the polaron-polaron model reduces to a competition between the direct antiferromagnetic carrier-carrier interactions characterized by  $J$ , and the indirect ferromagnetic carrier-ion-carrier interactions characterized by  $K'$ . By showing that there are circumstances in which the ferromagnetic interaction dominates, a theoretical justification for DMS ferromagnetism can be obtained. By applying the RS (Ryabchenko and Semenov) single step approximation and the interstitial approximation to the polaron-pair model, we have effectively separated the polaron-pair system into one mechanism for polaron formation and another for polaron-polaron interaction. It is this separation that makes possible a calculation of the polaron-pair partition function.

### III. PARTITION FUNCTION CALCULATION

To obtain the partition function for this problem, we must consider both the interacting part of the system (the carriers and magnetic ions within the polarons and the interstitial region), and the non-interacting part (those magnetic ions that are external to both the polarons and the interstitial region). Thus, the full partition function takes the form,  $Z = Z_{pp}Z_{ext}$ , where  $Z_{pp}$  is the polaron-pair partition function and  $Z_{ext}$  is the partition function of the non-interacting external ion spins.

Since the external ions are inert,  $Z_{ext}$  is just given by the degeneracy of the magnetic ion spins. Taking the magnetic ions to be spin-5/2 (as is the case for Mn), each spin has  $2s+1 = 6$  orientations. Therefore,  $Z_{ext} = 6^{N_{ext}}$ , where  $N_{ext}$ , the number of external magnetic ions in the system, is equal to the total number of ions in the system minus the number of ions in the polarons and interstitial region. Note that while these non-interacting external spins contribute no energy to the system, they contribute nonzero entropy and therefore cannot be neglected.

Due to the approximations made in developing our model, the polaron-pair system separates into an individual polaron part and a polaron-polaron interaction part. Hence, as will be explicitly shown, the polaron-pair partition function can be expressed as the product of two single polaron partition functions and a polaron-polaron interaction partition function.

#### A. Single Polaron Partition Function

The single polaron partition function can be calculated exactly for the single step model that we have adopted. For a single polaron, the Hamiltonian is

$$H = \lambda_s K \mathbf{s} \cdot \mathbf{S} = \frac{\lambda_s K}{2} [(\mathbf{s} + \mathbf{S})^2 - \mathbf{s}^2 - \mathbf{S}^2] \quad (3.1)$$

where  $\mathbf{s}$  is the carrier spin,  $\mathbf{S}$  is the sum of the magnetic ion spins within the polaron, and  $\lambda_s$  is a placeholder constant that has been inserted for notational convenience

and will eventually be set equal to one. For a given  $S$ , the total spin can take two values:  $S + \frac{1}{2}$  or  $S - \frac{1}{2}$ . The former yields an energy and degeneracy

$$E_+ = \frac{\lambda_s K S}{2} \quad g_+ = 2(S+1) \quad (3.2)$$

while the latter yields

$$E_- = -\frac{\lambda_s K(S+1)}{2} \quad g_- = 2S. \quad (3.3)$$

Thus, the single polaron partition function is given by

$$Z_{pol} = \text{Tr} [e^{-\beta H}] = \sum_S D(S) [g_+ e^{-\beta E_+} + g_- e^{-\beta E_-}] \quad (3.4)$$

where  $D(S)$  is the number of ways in which the ion spins can be arranged to give a collective spin  $S$ . Defining  $D_z(S)$  to be the number of ways that the ions can be arranged to give a collective z-component of spin equal to  $S$  and doing a bit of algebraic manipulation, we obtain

$$Z_{pol} = 2 \left[ 1 + (e^\gamma - 1) \frac{\partial}{\partial \gamma} \right] \sum_{S=-5N_1/2}^{5N_1/2} D_z(S) \cosh(\gamma S) \quad (3.5)$$

where  $\gamma \equiv \lambda_s \beta K / 2$  and  $N_1$  is the number of ion spins within the polaron. Using the definition of a delta-function,  $D_z(S)$  can be written as

$$D_z(S) = \text{Tr} \delta \left( S - \sum_{j=1}^{N_1} S_j^z \right) = \int_{-\infty}^{\infty} \frac{d\lambda}{2\pi} e^{i\lambda S} [6 F(i\lambda)]^{N_1} \quad (3.6)$$

where

$$F(x) = \frac{1}{6} \left[ e^{\frac{5x}{2}} + e^{\frac{3x}{2}} + e^{\frac{x}{2}} + e^{-\frac{x}{2}} + e^{-\frac{3x}{2}} + e^{-\frac{5x}{2}} \right]. \quad (3.7)$$

For large  $N_1$ , the sum over  $S$  can be converted to an integral and the partition function can be written as

$$Z_{pol} = 2 \left[ 1 + (e^\gamma - 1) \frac{\partial}{\partial \gamma} \right] \int_{-\infty}^{\infty} dS \times \int_{-\infty}^{\infty} \frac{d\lambda}{2\pi} (e^{\gamma S} + e^{-\gamma S}) e^{i\lambda S} [6 F(i\lambda)]^{N_1}. \quad (3.8)$$

Continuing to the imaginary temperature axis, using the definition of a delta-function, and continuing back to the real temperature axis, we obtain

$$Z_{pol} = 6^{N_1} Z_1 \quad Z_1 = 2 \left[ 1 + (e^\gamma - 1) \frac{\partial}{\partial \gamma} \right] F(\gamma)^{N_1} \quad (3.9)$$

where we have separated out the factor of  $6^{N_1}$  which will be cancelled by part of  $Z_{ext}$  in the full partition function. Note that this expression has the correct infinite temperature limit since  $Z_{pol}(T \rightarrow \infty) \rightarrow 2(6)^{N_1}$ , which is the partition function for a non-interacting system of  $N_1$  spin-5/2 magnetic ions and one spin-1/2 carrier.

### B. Polaron-Pair Partition Function

The exact quantum mechanical calculation of the polaron-pair partition function is significantly more complicated than the single polaron case. However, at low temperatures, a semiclassical technique introduced in Ref. 19 can be used to find  $Z_{pp}$  throughout the temperature range of interest. Specifically, we must make the assumption that the temperature is low enough such that the ion spins within the polarons and interstitial region are well enough aligned that the two polaron spins,  $S_1$  and  $S_2$ , and the interstitial region spin,  $S_3$ , are large enough to be treated as classical magnetic moments. Thus, we make a semiclassical approximation in which  $S_1$ ,  $S_2$ , and  $S_3$  are treated as classical spins while the carrier spins,  $s_1$  and  $s_2$ , are treated quantum mechanically. For the case we are interested in, appropriate for light to moderately doped II-VI based DMS, we expect that  $K', J \ll K$ . Consequently, we will first find the partition function for the case of non-interacting polarons ( $K' = J = 0$ ) and then include the effects of nonzero  $K'$  and  $J$  as first order perturbations. Separating the Hamiltonian into three parts, we write  $H = H_0 + H_1 + H_2$  where

$$\begin{aligned} H_0 &= K [\lambda_{s1}(\mathbf{s}_1 \cdot \mathbf{S}_1) + \lambda_{s2}(\mathbf{s}_2 \cdot \mathbf{S}_2)] \\ H_1 &= J(\mathbf{s}_1 \cdot \mathbf{s}_2) \\ H_2 &= K' [\lambda_{c1}(\mathbf{s}_1 \cdot \mathbf{S}_3) + \lambda_{c2}(\mathbf{s}_2 \cdot \mathbf{S}_3)] \end{aligned} \quad (3.10)$$

and we have introduced four new constants,  $\lambda_{s1}$ ,  $\lambda_{s2}$ ,  $\lambda_{c1}$ , and  $\lambda_{c2}$ . While these constants will be set equal to unity at the end of our calculation, they act as placeholders which will be useful when we optimize our model parameters in Sec. IV.

In the non-interacting polarons limit ( $K' = J = 0$ ), the polaron-pair partition function is simply  $Z_{pp} = 6^{N_1+N_2} Z_1 Z_2$  where  $Z_1$  and  $Z_2$  are the single polaron partition functions given by Eq. 3.9 with  $\gamma_1 = \lambda_{s1}\beta K/2$  and  $\gamma_2 = \lambda_{s2}\beta K/2$  respectively. In the semiclassical limit, the wave functions of the non-interacting polaron-pair are:  $\alpha(1)\alpha(2)$ ,  $\alpha(1)\beta(2)$ ,  $\beta(1)\alpha(2)$ , and  $\beta(1)\beta(2)$ , where  $\alpha$  is the total spin  $S + 1/2$  state of the single polaron (carrier and magnetic ions aligned) and  $\beta$  is the  $S - 1/2$  state (carrier and magnetic ions anti-aligned). At the low temperatures for which the semiclassical approximation is valid, only the ground state,  $\beta(1)\beta(2)$ , is significantly occupied. Hence, the  $K'$  and  $J$  perturbations are taken to be the diagonal matrix elements in this ground state.

Therefore, for interacting polarons with nonzero  $K'$  and  $J$ , we write

$$M_J = \langle \beta(1)\beta(2) | H_1 | \beta(1)\beta(2) \rangle = \frac{J \mathbf{S}_1 \cdot \mathbf{S}_2}{4 S_1 S_2} = \frac{J \mu_{12}}{4} \quad (3.11)$$

$$\begin{aligned} M_{K'} &= \langle \beta(1)\beta(2) | H_2 | \beta(1)\beta(2) \rangle \\ &= -\frac{K'}{2} \left[ \frac{\lambda_{c1} S_2 \mathbf{S}_1 + \lambda_{c2} S_1 \mathbf{S}_2}{S_1 S_2} \cdot \mathbf{S}_3 \right] = -\frac{\Omega}{\beta} \mu_3 \mathbf{S}_3 \end{aligned} \quad (3.12)$$

where

$$\Omega = \frac{\beta K'}{\sqrt{2}} \sqrt{\frac{\lambda_{c1}^2 + \lambda_{c2}^2}{2} + \lambda_{c1} \lambda_{c2} \mu_{12}}, \quad (3.13)$$

$\mu_{12}$  is the cosine of the angle between  $S_1$  and  $S_2$ , and  $\mu_3$  is the cosine of the angle between  $S_3$  and the z-axis. Making use of these matrix elements, the polaron-pair partition function can be written as

$$\begin{aligned} Z_{pp} &= \text{Tr} \left[ e^{-\beta(H_0 + M_J + M_{K'})} \right] = \int d^3 S_1 d^3 S_2 d^3 S_3 \\ &\times D(S_1) D(S_2) D(S_3) e^{\gamma_1 S_1 + \gamma_2 S_2 - \frac{\beta J}{4} + \Omega \mu_3 S_3}. \end{aligned} \quad (3.14)$$

Performing the indicated integration and doing a bit of algebra this becomes

$$Z_{pp} = 6^{N_1+N_2} Z_1 Z_2 \int_0^{\sqrt{2}} e^{-\frac{\beta J(x^2-1)}{4}} [6 F(\Omega)]^{N_3} x dx \quad (3.15)$$

where  $x^2 = 1 + \mu_{12}$ ,  $N_3$  is the number of magnetic ion spins within the interstitial region, and we have identified  $Z_1$  and  $Z_2$  as the single polaron partition functions. Notice that in this approximation, the partition function does separate into a polaron formation factor and a polaron-polaron interaction factor. Multiplying this result by the partition function for external ion spins,  $Z_{ext} = 6^{N_{tot} - N_1 - N_2 - N_3}$ , and dropping the constant factor of  $6^{N_{tot}}$ , we obtain the full partition function

$$Z = Z_1 Z_2 Z_3 \quad Z_3 = \int_0^{\sqrt{2}} e^{-\frac{\beta J(x^2-1)}{4}} F(\Omega)^{N_3} x dx \quad (3.16)$$

where  $Z_3$  is the polaron-polaron interaction part.

### IV. VARIATIONAL OPTIMIZATION OF MODEL PARAMETERS

Given the partition function calculated in the previous section, we proceed to optimize the parameters of our model via a variational approach. At  $T = 0$ , optimal values of the model parameters could be obtained by

minimizing the expectation value of the model Hamiltonian. At  $T \neq 0$ , we adopt an analogous variational approach described by Feynman<sup>25</sup> for which the quantity to be minimized is the  $\mathcal{F}$ -function

$$\mathcal{F} \equiv F_m + \langle H - H_m \rangle \quad (4.1)$$

where  $H_m$  is the model Hamiltonian and  $H$  is the true hamiltonian. The average  $\langle \dots \rangle$  is taken over the states of  $H_m$ .  $\mathcal{F}$  can be shown<sup>25</sup> to be an upper bound on the true free energy  $F$  of the Hamiltonian  $H$  at the temperature  $T$  in question. By minimizing  $\mathcal{F}$  with respect to the model parameters, optimal values can be determined as a function of temperature.

As will be shown explicitly in Sec. IV B, the total  $\mathcal{F}$ -function separates into the sum of two single polaron functions and a polaron-polaron interaction function. Therefore, we shall optimize the single polaron parameters first and then consider the interaction parameters.

### A. Single Polaron Parameter Optimization

The single polaron  $\mathcal{F}$ -function can be obtained by expressing  $\langle H_m \rangle$ ,  $\langle H \rangle$ , and  $F_m$  in terms of the single polaron partition function,  $Z_1$ . Recall that the model Hamiltonian has the form

$$H_m = \lambda_s K \sum_j \mathbf{s} \cdot \mathbf{S}_j \quad (4.2)$$

where index  $j$  runs over all magnetic ion spins,  $\mathbf{S}_j$ , within a sphere of radius  $R$  about the carrier spin,  $\mathbf{s}$ , and  $\lambda_s$  is a constant which will soon be set equal to unity. Taking the thermal average over the eigenstates of  $H_m$  yields that

$$\langle H_m \rangle = \lambda_s K N_1 \langle \mathbf{s} \cdot \mathbf{S}_j \rangle = -\frac{\lambda_s}{\beta} \frac{\partial \ln Z_1}{\partial \lambda_s} \quad (4.3)$$

where  $N_1$  is the number of magnetic ions within the polaron. The true Hamiltonian has the form

$$H = \alpha \sum_n \mathbf{s} \cdot \mathbf{S}_n |\Psi_n|^2 \quad (4.4)$$

where the index  $n$  runs over all magnetic ion spins. Therefore, noting that  $\langle \mathbf{s} \cdot \mathbf{S}_n \rangle$  is only nonzero for ion spins within the polaron, we find that

$$\langle H \rangle = \alpha \sum_j |\Psi_j|^2 \langle \mathbf{s} \cdot \mathbf{S}_j \rangle = -\frac{\gamma_s}{\beta} \frac{\partial \ln Z_1}{\partial \lambda_s} \quad (4.5)$$

where

$$\gamma_s = \frac{\alpha}{KV_s} \int_S d^3r |\Psi(r)|^2 \quad (4.6)$$

and the integral is over a sphere of radius  $R$  and volume  $V_s$ . Finally, since the free energy is

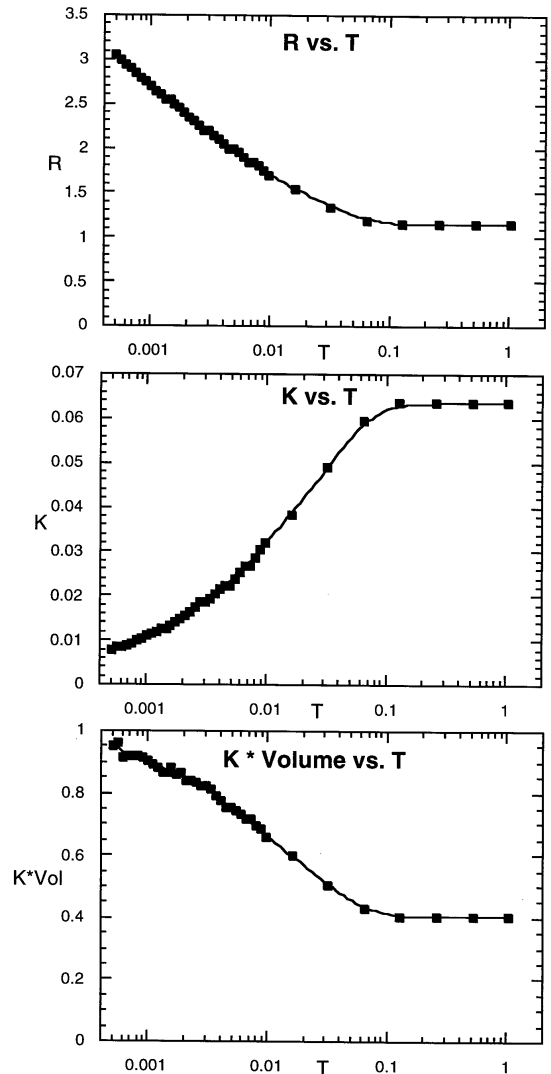


FIG. 4. Temperature dependence of single polaron parameters. All distances are in units of  $a_B$  and all energies are in units of  $\alpha/a_B^3 \sim 625$  K.

$$F_m = -\frac{1}{\beta} \ln Z_1 \quad (4.7)$$

we can combine the expressions above (setting  $\lambda_s = 1$ ) to obtain the single polaron  $\mathcal{F}$ -function

$$\mathcal{F}_1 = -\frac{1}{\beta} \left[ \ln Z_1 + (\gamma_s - 1) \frac{\partial \ln Z_1}{\partial \lambda_s} \right] \quad (4.8)$$

where  $Z_1$  is given by Eq. (3.9). By minimizing  $\mathcal{F}_1$  with respect to the parameters  $R$  and  $K$ , the optimal values of these parameters can be found.

Performing such a procedure numerically over a range of temperature values, the optimal values of the single polaron parameters were determined as functions of temperature. The results of this optimization for a magnetic

ion density of 5 ions per sphere of radius  $1a_B$  are plotted in Fig. 4.

In the high temperature limit ( $T \gg K$ ), the exchange interaction between the carrier and the magnetic ions within the polaron is insignificant compared to temperature. Thus, the magnetic ion spins are not aligned and there is no difference between the free energy of a spin within the polaron and that of an external spin. As a result, the  $\mathcal{F}$ -function is minimized when the model carrier wave function best matches the true carrier wave function. This matching of a step of width  $R$  and height  $K$  to a hydrogenic wave function yields the optimal, temperature-independent values of  $R$  and  $K$ . Thus, as is shown in Fig. 4,  $R$ ,  $K$ , and  $KV_s$  (the total exchange energy) are temperature-independent in the high temperature regime.

For low temperatures ( $T \ll K$ ), the carrier-ion exchange interaction is significant compared to temperature. Thus, the magnetic ion spins located near the carrier anti-align with the carrier spin. In this situation, the inclusion of an additional ion within the polaron entails a gain in exchange energy. However, since the number of external spins decreases by one, there is also a decrease in the entropy of free spins. Therefore, the optimal  $R$  is determined by the balance of exchange energy and the entropy of free spins. As  $T$  decreases, the exchange energy gained by increasing the size of the polaron becomes more valuable. Thus, as is shown in Fig. 4,  $R$  increases as  $\log(1/T)$  as  $T$  drops. As  $R$  increases,  $K$  must decrease in order to maintain the match between the model step wave function and the true wave function. Thus,  $K$  decreases with decreasing  $T$ . Finally, despite the decrease in  $K$ , the total exchange energy (which is proportional to  $KV_s$ ) increases as  $T$  drops and the spins align.

It is interesting to note that in this problem, the variational principle leads one to match the Hamiltonian at *high*  $T$ , while entropy-energy balance determines the parameters at *low*  $T$ . This is just the converse of what one expects in most problems.

## B. Polaron-Pair Parameter Optimization

Just as for the single polaron, we can obtain the polaron-pair  $\mathcal{F}$ -function by expressing  $\langle H_m \rangle$ ,  $\langle H \rangle$ , and  $F_m$  in terms of the full partition function,  $Z$ . For the polaron-pair, our model Hamiltonian is

$$\begin{aligned} H_m = & \lambda_{s1} K \sum_i \mathbf{s}_1 \cdot \mathbf{S}_i + \lambda_{s2} K \sum_j \mathbf{s}_2 \cdot \mathbf{S}_j \\ & + \lambda_{c1} K' \sum_k \mathbf{s}_1 \cdot \mathbf{S}_k + \lambda_{c2} K' \sum_k \mathbf{s}_2 \cdot \mathbf{S}_k + J \mathbf{s}_1 \cdot \mathbf{s}_2 \end{aligned} \quad (4.9)$$

where indices  $i$  and  $j$  run over the magnetic ions in polaron 1 and 2 respectively,  $k$  runs over ions in the cylindrically symmetric interstitial region, and the  $\lambda$ 's are con-

stants which will soon be set equal to one. Taking the thermal average then yields

$$\begin{aligned} \langle H_m \rangle = & \lambda_{s1} K N_1 \langle \mathbf{s}_1 \cdot \mathbf{S}_i \rangle + \lambda_{s2} K N_2 \langle \mathbf{s}_2 \cdot \mathbf{S}_j \rangle \\ & + \lambda_{c1} K' N_3 \langle \mathbf{s}_1 \cdot \mathbf{S}_k \rangle + \lambda_{c2} K' N_3 \langle \mathbf{s}_2 \cdot \mathbf{S}_k \rangle \\ & + J \langle \mathbf{s}_1 \cdot \mathbf{s}_2 \rangle \end{aligned} \quad (4.10)$$

where  $N_1 = N_2$  are the number of ions in polaron 1 and 2, and  $N_3$  is the number of ions in the interstitial region. Noting that

$$\begin{aligned} \langle \mathbf{s}_1 \cdot \mathbf{S}_i \rangle = \langle \mathbf{s}_2 \cdot \mathbf{S}_j \rangle = & -\frac{1}{K N_1} \frac{1}{\beta} \frac{\partial \ln Z}{\partial \lambda_{s1}} \\ \langle \mathbf{s}_1 \cdot \mathbf{S}_k \rangle = \langle \mathbf{s}_2 \cdot \mathbf{S}_k \rangle = & -\frac{1}{K' N_3} \frac{1}{\beta} \frac{\partial \ln Z}{\partial \lambda_{c1}} \end{aligned} \quad (4.11)$$

and setting the  $\lambda$ 's equal to one, this becomes

$$\langle H_m \rangle = -\frac{2}{\beta} \left[ \frac{\partial \ln Z}{\partial \lambda_{s1}} + \frac{\partial \ln Z}{\partial \lambda_{c1}} \right] + J \langle \mathbf{s}_1 \cdot \mathbf{s}_2 \rangle. \quad (4.12)$$

Since the true Hamiltonian has the form

$$H = \alpha \sum_n \mathbf{s}_1 \cdot \mathbf{S}_n |\Psi_{1n}|^2 + \alpha \sum_n \mathbf{s}_2 \cdot \mathbf{S}_n |\Psi_{2n}|^2 + J \mathbf{s}_1 \cdot \mathbf{s}_2 \quad (4.13)$$

and we know that  $\langle \mathbf{s} \cdot \mathbf{S}_n \rangle$  is only nonzero for ion spins within the polarons or interstitial region

$$\begin{aligned} \langle H \rangle = & \alpha \langle \mathbf{s}_1 \cdot \mathbf{S}_i \rangle \sum_i |\Psi_{1i}|^2 + \alpha \langle \mathbf{s}_1 \cdot \mathbf{S}_k \rangle \sum_k |\Psi_{1k}|^2 \\ & + \alpha \langle \mathbf{s}_2 \cdot \mathbf{S}_j \rangle \sum_j |\Psi_{2j}|^2 + \alpha \langle \mathbf{s}_2 \cdot \mathbf{S}_k \rangle \sum_k |\Psi_{2k}|^2 \\ & + J \langle \mathbf{s}_1 \cdot \mathbf{s}_2 \rangle. \end{aligned} \quad (4.14)$$

Again making use of Eq. (4.11), this becomes

$$\langle H \rangle = -\frac{2}{\beta} \left[ \gamma_s \frac{\partial \ln Z}{\partial \lambda_{s1}} + \gamma_c \frac{\partial \ln Z}{\partial \lambda_{c1}} \right] + J \langle \mathbf{s}_1 \cdot \mathbf{s}_2 \rangle \quad (4.15)$$

where  $\gamma_s$  is defined in Eq. (4.6) and we have now defined

$$\gamma_c = \frac{\alpha}{K V_c} \int_C d^3 r |\Psi_1(r)|^2 \quad (4.16)$$

where the integral is over the cylindrically symmetric interstitial region of volume  $V_c$ . Subtracting Eq. (4.12) from Eq. (4.15) and adding the free energy,  $F_m = -\frac{1}{\beta} \ln Z$ , we obtain the polaron-pair  $\mathcal{F}$ -function

$$\mathcal{F} = -\frac{1}{\beta} \left[ \ln Z + 2(\gamma_s - 1) \frac{\partial \ln Z}{\partial \lambda_{s1}} + 2(\gamma_c - 1) \frac{\partial \ln Z}{\partial \lambda_{c1}} \right] \quad (4.17)$$

where  $Z$  is the partition function given by Eq. (3.16). Since  $Z$  is of the form  $Z = Z_1 Z_2 Z_3$ , it is clear that  $\mathcal{F}$  is of the form  $\mathcal{F} = \mathcal{F}_1 + \mathcal{F}_2 + \mathcal{F}_3$  and therefore separates

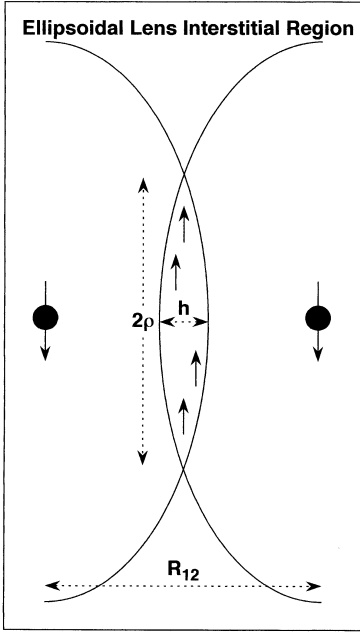


FIG. 5. Schematic of ellipsoidal lens shaped interstitial region.

into a polaron formation term,  $\mathcal{F}_1 + \mathcal{F}_2 = 2\mathcal{F}_1$ , which we developed in the previous section, and a polaron-polaron interaction term

$$\mathcal{F}_3 = -\frac{1}{\beta} \left[ \ln Z_3 + 2(\gamma_c - 1) \frac{\partial \ln Z_3}{\partial \lambda_{c1}} \right]. \quad (4.18)$$

Since these terms share no variational parameters, the polaron-pair model can be optimized by using  $\mathcal{F}_1$  to optimize  $K$  and  $R$  (as we did in the previous section) and using  $\mathcal{F}_3$  to optimize  $K'$  and the parameters describing the geometry of the interstitial region.

Before we can proceed to minimize  $\mathcal{F}_3$ , we must define a specific geometry for the interstitial region between the two polarons. The bi-spherical geometry of the problem suggests that a natural choice would be the spherical lens formed by the intersection of two spheres centered on the two polarons. However, such a shape can be completely specified by a single parameter, the lens width  $h$ . In order to provide an additional degree of freedom within the model, we will use the slightly more general ellipsoidal lens formed by the intersection of two ellipsoids centered on the polarons. In this manner, the interstitial region can be specified by two parameters, the lens width,  $h$ , and the lens radius,  $\rho$ . The details of this shape are depicted in Fig. 5.

The task of optimizing the model parameters,  $K'$ ,  $h$ , and  $\rho$ , is complicated in two ways. First of all, unlike the single polaron case where both the partition function,  $Z_1$ , and the geometrical factor,  $\gamma_s$ , could be obtained analytically, both the interaction partition function,  $Z_3$ , and the interstitial geometrical factor,  $\gamma_c$ , must be calculated

numerically. This complicates the numerics but poses no fundamental problem.

The second complication requires a bit more attention. Naively one would expect that by blindly varying these three parameters until  $\mathcal{F}_3$  is minimized, the optimal values of these parameters could be obtained. However, upon closer examination, it becomes clear that this is not the case. In performing this optimization of the interstitial region parameters, it is our objective to determine the parameters that best match the true interaction between *both* carriers and the magnetic ions in the interstitial region. However, minimizing the  $\mathcal{F}$ -function merely yields the configuration that, overall, is most energetically favorable. As a result, if all three parameters are varied, the minimum  $\mathcal{F}_3$  will be achieved when the interstitial region has totally engulfed both of the polarons. In this configuration, the interstitial region contains ions that are very close to the carriers and therefore experience large exchange interactions. However, these ions that interact very strongly with one of the polarons barely interact at all with the other. Thus, the result of an unconstrained minimization does not yield an interstitial region with which *both* of the carriers interact strongly. Therefore, to obtain sensible results, the minimization of the interaction  $\mathcal{F}$ -function must be constrained. Two methods of constraining the minimization have been developed: the fixed width method and the optimally spherical method.

The interstitial region in which both carrier wave functions are significant must be concentrated about the point halfway between the two polarons. Thus, one method of constraining the minimization of the  $\mathcal{F}$ -function is to fix the lens width,  $h$ , to a set value. Using this fixed width method, the only parameters that are allowed to vary are the interstitial interaction strength,  $K'$ , and the lens radius,  $\rho$ . For a given temperature, the  $\mathcal{F}$ -function will be minimized for some optimal values of these two parameters. Thus, by performing a numerical minimization for a range of temperature values, the temperature dependence of  $K'$  and  $\rho$  can be determined.

In the fixed width model, the fixed value of  $h$  is chosen such that both carrier wave functions will be “significant” within the interstitial region. In a sense, the choice of a particular  $h$  defines the threshold of exchange interaction strength with both carriers that is required for an ion to be included in the interstitial region. However, as temperature changes, this threshold should change as well since all energies in the system are measured with respect to temperature. Thus, as temperature drops, the threshold should also drop and the width of the interstitial region should increase (to include those additional ions that now meet the lowered threshold). This is a feature that is not incorporated into the fixed width method, since  $h$  remains constant as temperature varies. Unfortunately, this problem cannot be solved by making  $h$  a variational parameter since, if this is the case, the minimum  $\mathcal{F}$ -function will only be achieved when the interstitial region engulfs the polarons. One way to incorpo-

rate the growth of  $h$  with decreasing  $T$  into the process would be to choose a new fixed  $h$  for every  $T$  and set the temperature-dependent threshold for inclusion in the interstitial region by hand. However, this approach would require a prior knowledge of the temperature dependence of  $h$ , which we do not have.

A more natural way to allow the threshold to vary with  $T$  is to let the threshold be set by the geometry of the system. The polaron-pair problem consists of two sources of radially symmetric wave functions separated by an inter-impurity distance. Thus, the system has an innate bi-spherical geometry. If one were to define a region in space in which the wave functions of both carriers would surpass a given threshold, the geometry of the system and the spherically symmetric nature of the wave functions would dictate that this region be the intersection of two spheres centered at the carrier sites – a spherical lens. Therefore, the natural shape for the interstitial region is a spherical lens. This fact provides the condition for setting the width of the interstitial region in what we call the optimally spherical method. For a given temperature, the fixed width,  $h$ , is set to be that for which the minimization of the  $\mathcal{F}$ -function automatically yields a value of the lens radius,  $\rho$ , for which the ellipsoidal lens becomes spherical. Thus, the result is a spherical lens interstitial region in which the lens radius is the energetically optimal radius for the given width. As we will show, this technique yields the proper increase in  $h$  as temperature drops.

Using both the fixed width approach (with  $h$  set to  $2a_B$ ) and the optimally spherical approach, the polaron-polaron interaction parameters,  $K'$ ,  $h$ , and  $\rho$ , were optimized as functions of temperature. The results of this optimization for a magnetic ion density of 5 ions per sphere of radius  $1a_B$  and a carrier density such that  $R_{12} = 6a_B$  are plotted in Fig. 6. Although the parameter values are plotted over a wide range of temperatures, they are only meaningful for temperatures at which the polaron-pair model is valid. Clearly, once the polarons have increased to a size such that they touch the interstitial region, the polaron-pair model is no longer valid. This impact between the polarons and the interstitial region occurs at  $T = T_{\text{impact}}$  where  $2R + h = R_{12}$ . In Fig. 6, the temperature of impact has been denoted by a vertical dashed line for both the fixed width and the optimally spherical cases. Note that for either method,  $T_{\text{impact}}$  is found to be approximately equal to  $0.005 \alpha/a_B^3$  or around 3 K for typical ion and carrier densities. Since  $K'(T_{\text{impact}}) \ll T_{\text{impact}}$ , this cutoff temperature lies within the high temperature regime ( $T \gg K'$ ) where the interstitial ion-carrier interactions are insignificant compared to temperature. Hence, for temperatures where our model is well defined, all of the polaron-polaron interaction parameters are constant. For very low temperatures ( $T \ll K'$ ), our results are not quantitative, but since polarons are nearly aligned (either parallel or antiparallel) by this point, this regime lies beyond the temperature range of interest. The use of a constant pa-

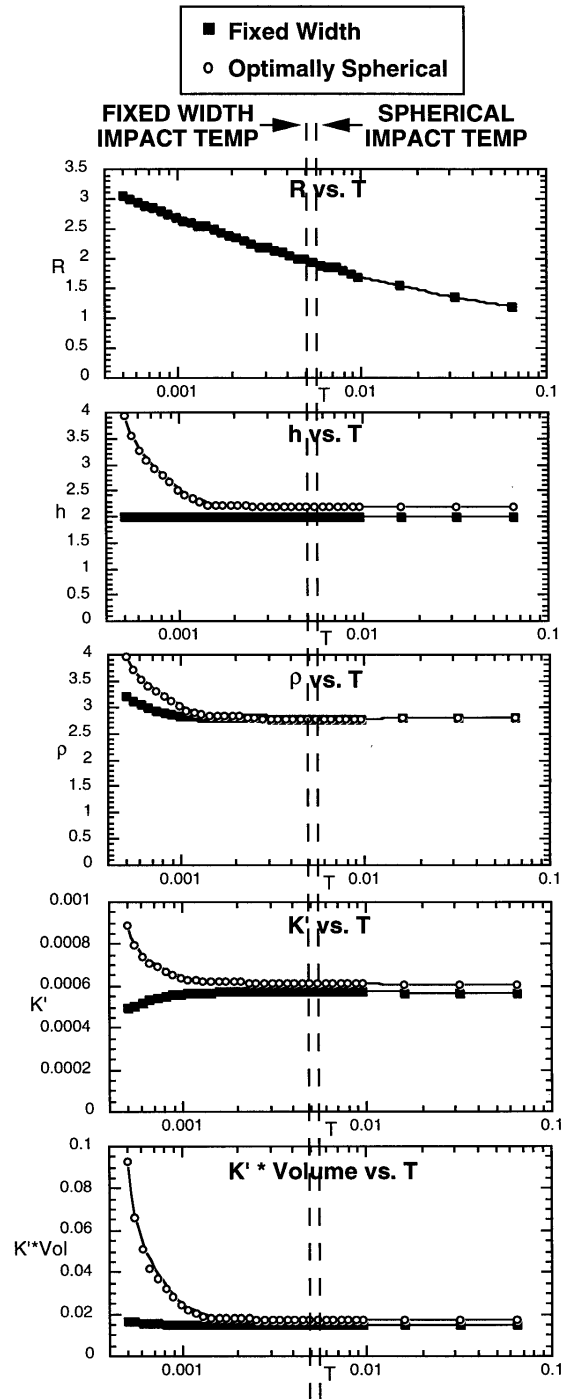


FIG. 6. Temperature dependence of polaron-polaron interaction parameters obtained using both the fixed width and optimally spherical methods of constraining the minimization. All distances are in units of  $a_B$  and all energies are in units of  $\alpha/a_B^3 \sim 625$  K.

parameter model to treat the polaron-polaron interaction in Ref. 19 is therefore justified.

## V. POLARON-POLARON INTERACTION

Given the polaron-polaron interaction partition function,  $Z_3$ , as expressed in Eq. (3.16), it follows that the thermal average of the cosine of the angle between the two polaron spins can be obtained via

$$\langle \cos \theta_{12} \rangle = \frac{\int_0^{\sqrt{2}} (x^2 - 1) e^{-\frac{J(x^2-1)}{4k_B T}} F\left(\frac{K'x}{\sqrt{2k_B T}}\right)^{N_3} x dx}{\int_0^{\sqrt{2}} e^{-\frac{J(x^2-1)}{4k_B T}} F\left(\frac{K'x}{\sqrt{2k_B T}}\right)^{N_3} x dx} \quad (5.1)$$

where  $F(z)$  is defined in Eq. (3.7),  $x^2 - 1 = \cos \theta_{12}$ , and  $N_3 = N_3(h, \rho)$  is the number of magnetic ions in the interstitial region. As motivated above, the polaron-polaron interaction parameters,  $K'$  and  $N_3$ , are approximately temperature-independent in the temperature range of interest. Thus, for various constant values of  $J$ ,  $K'$ , and  $N_3$ , the above expression can be evaluated numerically as a function of temperature to reveal the temperature dependence of the inter-polaron angle. The results have been plotted in Fig. 7 for  $N_3 = 20$  and several values of the ratio  $K'/J$ . We see that for reasonable parameter values,  $\langle \cos \theta_{12} \rangle$  is positive and neighboring polarons tend to align. For large enough  $K'/J$ , indirect ferromagnetic carrier-ion-carrier interactions can dominate the direct antiferromagnetic carrier-carrier interactions to yield a net ferromagnetic polaron-polaron interaction.

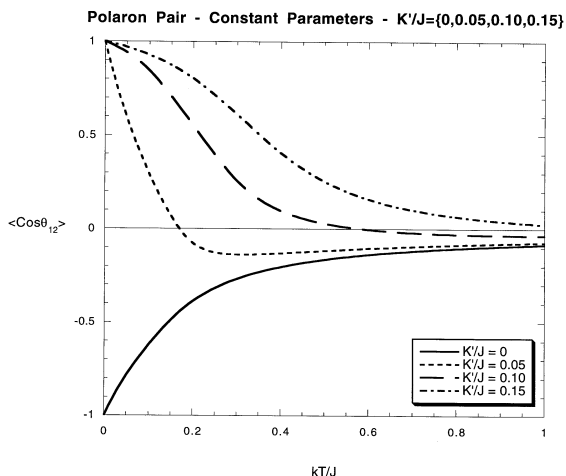


FIG. 7. Thermal average of the cosine of the angle between polaron spins,  $\langle \cos \theta_{12} \rangle$ , plotted versus temperature for  $N_3 = 20$  and several values of the ratio  $K'/J$ .

## VI. CONCLUSIONS

In this analysis of the magnetic behavior of diluted magnetic semiconductors, we have proposed a simplified model to describe both the formation of bound magnetic polarons and the interactions between them. Approximating carrier wave functions via sharp cutoffs that define polarons and interstitial regions between them, we have obtained a tractable model and calculated the resulting partition function. Utilizing a finite temperature variational approach, the model parameters have been optimized as functions of temperature. At very high temperatures ( $T \gg K$ ), the spins within the system are not aligned and the model parameters obtain the constant values for which the model wave functions best match the true wave functions. At lower temperatures ( $K' \ll T \ll K$ ), where the carrier-ion exchange interaction becomes more significant, both polaron size and total intra-polaron exchange energy increase logarithmically with decreasing  $T$ . However, throughout this intermediate temperature range, the parameters controlling polaron-polaron interactions,  $K'$ ,  $h$ , and  $\rho$ , remain constant as  $T$  varies. At very low temperatures ( $T \ll K'$ ), even these interstitial region parameters would become temperature dependent. However, for reasonable carrier and ion densities, the polarons grow large enough to touch the interstitial region, such that our model ceases to be valid, well before this regime is realized. Hence, for temperatures of interest, a model in which the polaron-polaron interaction parameters are constant is justified variationally. Therefore, for reasonable values of  $K'/J$  we obtain, as in Ref. 19, a net ferromagnetic polaron-polaron interaction, in agreement with the experimental evidence for ferromagnetism in insulating doped DMS.

The further growth of the polaron pair bubble, for  $T \ll K'$ , could be captured via a variational scheme employing an appropriately generalized object. Starting at the point of polaron overlap, such an object, involving two or three variational parameters, should evolve from a “peanut shape”, with cylindrical symmetry, to a sphere with the mid-point of the two dopant sites as its center. This could be a promising direction for future research.

Since this work was completed, a tendency toward ferromagnetism has been observed by other groups.<sup>26,27</sup> In addition, a separate mechanism for ferromagnetic alignment, resulting from the strong local exchange fields experienced at the two impurity sites due to nearby Mn, has been considered by Angelescu and Bhatt.<sup>14</sup>

## ACKNOWLEDGMENTS

The authors would like to thank NEC Research Institute for allowing us to reproduce, in Fig. 1, the susceptibility data measured by J. Liu. This work was supported by NSF DMR-9400362 and 9809483. ACD acknowledges

support from the Princeton Center for Complex Materials at the Princeton Materials Institute.

---

- <sup>1</sup> H. Ohno, *Science* **281**, 951 (1998)
- <sup>2</sup> G. A. Prinz, *Science* **282**, 1660 (1998)
- <sup>3</sup> F. Matsukura, H. Ohno, A. Shen, and Y. Sugawara, *Phys. Rev. B* **57**, R2037 (1998)
- <sup>4</sup> T. Dietl and H. Ohno, *Physica E* **9**, 185 (2001); T. Dietl, H. Ohno, and F. Matsukura, *Phys. Rev. B* **63**, 195205
- <sup>5</sup> B. Beschoten, P. Crowell, I. Malajovich, D. Awschalom, F. Matsukura, A. Shen, and H. Ohno, *Phys. Rev. Lett.* **83**, 3073 (1999)
- <sup>6</sup> H. Ohno, *J. Mag. Magn. Mat.* **200**, 110 (1999)
- <sup>7</sup> J. Szczytko, W. Mac, A. Twardowski, F. Maksukura, and H. Ohno, *Phys. Rev. B* **59**, 12935 (1999)
- <sup>8</sup> T. Dietl, J. Cibert, P. Kossacki, D. Ferrand, S. Tatarenko, A. Wasiela, Y. Merle d'aubigne, F. Matsukura, N. Akiba, and H. Ohno, *Physica E* **7**, 967 (2000)
- <sup>9</sup> J. König, H. H. Lin, and A. H. MacDonald, *Phys. Rev. Lett.* **84**, 5628 (2000); M. F. Yang, S. J. Sun, and M. C. Chang, *Phys. Rev. Lett.* **86**, 5636 (2001); J. König, H. H. Lin, and A. H. MacDonald, *Phys. Rev. Lett.* **86**, 5637 (2001); J. König, H. H. Lin, A. H. MacDonald, cond-mat/0010471
- <sup>10</sup> J. Schliemann, J. König, H. H. Lin, A. H. MacDonald, *Appl. Phys. Lett.* **78**, 1550 (2001)
- <sup>11</sup> R. N. Bhatt and X. Wan, *Int. J. Mod. Phys. C* **10**, 1459 (1999)
- <sup>12</sup> X. Wan and R. N. Bhatt, cond-mat/0009161
- <sup>13</sup> M. Berciu and R. N. Bhatt, *Phys. Rev. Lett.* **87**, 107203 (2001)
- <sup>14</sup> D. E. Angelescu and R. N. Bhatt, cond-mat/0012279
- <sup>15</sup> M. P. Kennett, M. Berciu, and R. N. Bhatt, cond-mat/0102315
- <sup>16</sup> J. Liu, TN 9300720043LN, NEC Research Institute, Princeton, NJ (Oct 19, 1993); J. Z. Liu, G. Lewen, P. Becla, and P. A. Wolff, *Bull. Am. Phys. Soc.* **39**, 402 (1994)
- <sup>17</sup> P. A. Wolff, "Theory of Bound Magnetic Polarons in Semimagnetic Semiconductors," in J. K. Furdyna and J. Kossut, *Semiconductors and Semimetals Vol. 25: Diluted Magnetic Semiconductors* (Academic Press, San Diego, 1988)
- <sup>18</sup> K. Andres, R. N. Bhatt, P. Goalwin, T. M. Rice, and R. E. Walstedt, *Phys. Rev. B* **24**, 244 (1981); R. N. Bhatt and P. A. Lee, *Phys. Rev. Lett.* **48**, 344 (1982)
- <sup>19</sup> P. A. Wolff, R. N. Bhatt, and A. C. Durst, *J. Appl. Phys.* **79**, 5196 (1996)
- <sup>20</sup> A. C. Durst, Princeton University Senior Thesis, Part I (1995, unpublished)
- <sup>21</sup> A. C. Durst, Princeton University Senior Thesis, Part II (1996, unpublished); A. C. Durst and R. N. Bhatt (in preparation)
- <sup>22</sup> A. Baldereschi and N. O. Lipari, *Phys. Rev. B* **8**, 2697 (1973)
- <sup>23</sup> S. M. Ryabchenko and Y. G. Semenov, *Sov. Phys. JETP* **57**, 825 (1983)
- <sup>24</sup> R. N. Bhatt and P. A. Wolff, *Bull. Am. Phys. Soc.* **40**, 268 (1995)
- <sup>25</sup> R. P. Feynman, *Statistical Mechanics: A Set of Lectures* (W. A. Benjamin, Inc., Reading, MA, 1972)
- <sup>26</sup> D. Ferrand *et al*, *Physica B* **284-288**, 1177 (2000)
- <sup>27</sup> M. Sawicki *et al*, Proc. of Conf. on II-VI Semiconductors, Bremen, Sept 2001 (to be published in *Phys. Stat. Solidi*)